SECTION I

IMPROVEMENT OF AGRONOMIC AND MICROBIAL TRAITS

1

INSIGHTS INTO THE STRUCTURE AND FUNCTION OF ACYL-CoA: DIACYLGLYCEROL ACYLTRANSFERASE

RODRIGO M.P. SILOTO, QIN LIU, AND RANDALL J. WESELAKE

Agricultural Lipid Biotechnology Program, Department of Agricultural, Food and Nutritional Science, University of Alberta, 4-10 Agriculture/Forestry Centre, Edmonton, Alberta, Canada T6G 2P5

XIAOHUA HE AND THOMAS MCKEON

Western Regional Research Center, United States Department of Agriculture, Albany, California 94710, USA

Biocatalysis and Biomolecular Engineering, Edited by Ching T. Hou and Jei-Fu Shaw

1.1 INTRODUCTION

Production of vegetable oils has been recognized as a rapidly developing field in plant biotechnology that goes beyond food-based applications. Many kinds of vegetable oils are used in soaps and cosmetics or converted to oleochemicals that are extensively used to replace petrochemicals in paints, plastics, fuels, and lubricants. The demand for biodegradable chemicals applied to industrial products has been increasing, and therefore a boost in the production of vegetable oils and fats is needed. Biotechnological approaches including traditional plant breeding and direct genome modification through genetic engineering are crucial tools to increase seed oil production without extending the area of crop cultivation, which has a direct impact on deforestation and competition with food production. Moreover, even a diminutive increase in seed oil content reflects in considerable profitability. Despite the unprecedented advances derived from molecular genetics and genomics research on the biochemical pathways of plant lipid metabolism in the last decade, the mechanisms regulating seed oil content are not fully understood. Many aspects of key enzymes are not yet determined even in model plants such as *Arabidopsis thaliana* (Hildebrand et al., 2008). For example, recent studies focusing on intracellular trafficking indicated that compartmentalization of enzyme activities within the endoplasmic reticulum (ER) membrane represents an additional mechanism adopted by plant cells to control oil production and may be essential for channeling of particular fatty acids into storage lipids (Dyer and Mullen, 2008).

Nevertheless, manipulation of genes involved in storage lipid biosynthesis has been used to increase accumulation of seed triacylglycerol (TAG), the main component of vegetable oils (Weselake, 2002). It was recently demonstrated that overexpression of plant and fungi genes encoding acyl-CoA:diacylglycerol acyltransferase (DGAT, EC 2.3.1.20), which catalyzes the final assembly of TAG, resulted in small but significant increases in seed oil content in canola and soybean tested under field conditions (Lardizabal et al., 2008; Weselake et al., 2008). Indeed, the level of DGAT activity in developing seeds seems to have a direct effect on the accumulation of TAG (Perry and Harwood, 1993; Cahoon et al., 2007). Surprisingly, little is known about the molecular mechanisms governing DGAT activity. The most basic information about structure and function of this enzyme is essential for rational designs to increase its performance in oilseeds and have a direct reflection in seed oil content. In view of the biotechnological importance of DGATs from plants and fungi, we summarize some of the structural and functional aspects of these enzymes with particular attention to membrane topology, functional polypeptide motifs, and subcellular localization. We use *in silico* approaches to compare the findings obtained with related enzymes in animals and prokaryotes.

1.2 DISCOVERY OF DGAT

The first proceedings reporting DGAT activity date from the 1950s (Weiss and Kennedy, 1956; Weiss et al., 1960), but the genes encoding DGATs were not isolated

until the late 1990s. The first *DGAT* cDNA was cloned by taking advantage of homology between an expressed sequence tag (EST) and an acyl-CoA:cholesterol acyltransferase (ACAT, EC 2.3.1.26), a related enzyme previously isolated by a complementation assay of mammalian cells devoid of cholesterol ester biosynthesis (Chang et al., 1993). The mouse (*Mus musculus*) *DGAT* gene isolated in 1998 encodes a protein, here referred to as MmDGAT1 that is 20% identical to mouse ACAT with the most conserved regions on the C-terminus portion of the enzyme (Cases et al., 1998). A plant *DGAT* gene was consequently isolated through the characterization of the locus *TAG1* in an *A. thaliana* EMS-induced mutant (AS11) with altered seed fatty acid composition and decreased DGAT activity (Katavic et al., 1995). The locus *TAG1* contains a 3.4-kb gene encoding a polypeptide showing 41% identity with MmDGAT1 (Zou et al., 1999). The polypeptide encoded by *TAG1* (AtDGAT1) exhibits DGAT activity when expressed in yeast and can complement DGAT function in AS11 (Jako et al., 2001). *DGAT* genes from fungi were identified through protein purification, an approach that was previously not successful with other DGATs, perhaps because of their membrane association. Polypeptides exhibiting DGAT activity were purified from lipid bodies of *Umbelopsis ramanniana*, formerly known as *Mortierella ramanniana* (Lardizabal et al., 2001). These *DGATs* shared little or apparently no homology with the previous *DGAT* genes, and therefore were classified as *DGAT2*. Curiously, genes homologous to *DGAT1* have not been found in fungi genomes, although it has been suggested that yeast *ACATs* (*ARE1* and *ARE2* in *Saccharomyces cerevisiae*) represent *DGAT1* orthologs in these organisms because they also display minor DGAT activity (Yen et al., 2008).

Several lines of evidence suggest that DGAT1 belongs to a class of enzymes with acyl-CoA transferase activity, which can utilize different acceptors in addition to diacylglycerols. For example, MmDGAT1 also possesses acyl-CoA:retinol acyltransferase (ARAT, EC 2.6.1.57) activity (Yen et al., 2005), while an *A. thaliana* acyl-CoA:fatty alcohol acyltransferase (wax ester synthase, WSD1) also displays DGAT activity *in vitro* (Li et al., 2008). In the case of DGAT2, a similar scenario is observed. In animals, *DGAT2* belongs to a gene family with seven members in humans (Cases et al., 2001). Three of these genes encode polypeptides with acyl-CoA monoacylglycerol acyltransferase (MGAT, EC 2.3.1.22) activity (Yen et al., 2002; Yen and Farese, 2003; Cheng et al., 2003). Two additional members display acyl-CoA:wax alcohol acyltransferase (AWAT, EC 2.3.1.75) activity, which is analogous to WSD1 (Turkish et al., 2005).

Orthologs of *DGAT1* and *DGAT2* have been identified through DNA homology in many other organisms and are widely distributed in eukaryotes. Currently, a relatively wide collection of *DGAT* genes is available which facilitates more detailed studies of enzyme structure and function through bioinformatic approaches. Many of these genes have been functionally characterized in recombinant systems as described in Table 1.1.

In prokaryotes, a bifunctional WS/DGAT was identified in *Acinetobacter calcoaceticus* (Kalscheuer and Steinbuchel, 2003). WS/DGAT has no sequence similarity to DGAT1, DGAT2, or any of the related acyltransferases from eukaryotes. Another nonhomologous DGAT, referred to as AhDGAT, was characterized in peanuts

TABLE 1.1 Eukaryotic DGATs Functionally Tested in Recombinant Organisms

cDNA	Original Organism	Host Used for Expression and Relevant Genetic Markers	Reference
HsDGAT1	*H. sapiens*	*S. cerevisiae* 12501 (*dga1*$^{-}\Delta$)	Inokoshi et al. (2009)
AtDGAT1	*A. thaliana*	*B. napus*	Weselake et al. (2008)
BnDGAT1	*B. napus*	*B. napus*	Weselake et al. (2008)
TmDGAT1	*T. majus*	*S. cerevisiae* H1246 (*are1*$^{-}\Delta$, *are2*$^{-}\Delta$, *dga1*$^{-}\Delta$, *lro1*$^{-}\Delta$), *A. thaliana* and *B. napus*	Xu et al. (2008)
ZmDGAT1	*Z. mays*	*Z. mays* and *S. cerevisiae* (*dga1*$^{-}\Delta$, *lro1*$^{-}\Delta$)	Zheng et al. (2008)
VgDGAT1	*V. galamensis*	*S. cerevisiae*	Yu et al. (2008)
VfDGAT1	*V. fordii*	*S. cerevisiae* SCY1998 (*dga1*$^{-}\Delta$, *lro1*$^{-}\Delta$)	Shockey et al. (2006)
AhDGAT	*A. hypogaea*	*E. coli*	Saha et al. (2006)
MmDGAT1	*M. musculus*	COS7-cells (*C. sabaeus*)	Yen et al. (2005)
EaDGAT1	*E. alatus*	*S. cerevisiae* H1266 (*are2*$^{-}\Delta$, *dga1*$^{-}\Delta$, *lro1*$^{-}\Delta$)	Milcamps et al. (2005)
AtDGAT1	*A. thaliana*	*S. cerevisiae* H1266 (*are2*$^{-}\Delta$, *dga1*$^{-}\Delta$, *lro1*$^{-}\Delta$)	Milcamps et al. (2005)
RcDGAT1	*R. communis*	*S. cerevisiae*	He et al. (2004)
TgDGAT1	*T. gondii*	*S. cerevisiae* SCY910 (*are1*$^{-}\Delta$, *are2*$^{-}\Delta$)	Quittnat et al. (2004)
HsDGAT1	*H. sapiens*	McA-RH7777 cells (*R. norvegicus*)	Liang et al. (2004)
BnDGAT1	*B. napus*	*P. pastoris*	Nykiforuk et al. (2002)
MmDGAT1	*M. musculus*	Sf9 insect cells (*S. frugiperda*)	Cases et al. (2001)
AtDGAT1	*A. thaliana*	*A. thaliana* AS11	Jako et al. (2001)
AtDGAT1	*A. thaliana*	*S. cerevisiae* SCY 062	Bouvier-Nave et al. (2000a)
CeDGAT1	*C. elegans*	*S. cerevisiae* SCY 062	Bouvier-Nave et al. (2000a)
NtDGAT1	*N. tabacum*	*S. cerevisiae* SCY 062	Bouvier-Nave et al. (2000a)
AtDGAT1	*A. thaliana*	*S. cerevisiae* SCY059 (*are1*$^{-}\Delta$, *are2*$^{-}\Delta$), *N. tabacum*	Bouvier-Nave et al. (2000b)
AtDGAT1	*A. thaliana*	Sf21 insect cells (*S. frugiperda*)	Hobbs et al. (1999)
AtDGAT1	*A. thaliana*	*S. cerevisiae* YMN5 (*Slc1*$^{-}\Delta$)	Zou et al. (1999)
MmDGAT1	*M. musculus*	H5 insect cells (*T. ni*)	Cases et al. (1998)
HsDGAT2	*H. sapiens*	*S. cerevisiae* 12501 (*dga1*$^{-}\Delta$)	Inokoshi et al. (2009)
RcDGAT2	*R. communis*	*A. thaliana* and *S. cerevisiae* (*dga1*$^{-}\Delta$)	Burgal et al. (2008)
UeDGAT2	*U. ramanniana*	*G. max*	Lardizabal et al. (2008)

TABLE 1.1 (*Continued*)

cDNA	Original Organism	Host Used for Expression and Relevant Genetic Markers	Reference
RcDGAT2	*R. communis*	*S. cerevisiae*	Kroon et al. (2006)
MmDGAT2	*M. musculus*	COS7-cells (*C. sabaeus*)	Stone et al. (2006)
VfDGAT2	*V. fordii*	*S. cerevisiae* SCY1998 (*dga1*$^{-}\Delta$, *lro1*$^{-}\Delta$)	Shockey et al. (2006)
HsDGAT2	*H. sapiens*	*S. cerevisiae* ScY2051 (*are2*$^{-}\Delta$, *dga1*$^{-}\Delta$, *lro1*$^{-}\Delta$)	Turkish et al. (2005)
MmDGAT2	*M. musculus*	Sf9 insect cells (*S. frugiperda*)	Cases et al. (2001)
HsDGAT2	*H. sapiens*	Sf9 insect cells (*S. frugiperda*)	Cases et al. (2001)
CeDGAT2	*C. elegans*	Sf9 insect cells (*S. frugiperda*)	Lardizabal et al. (2001)
ScDGAT2	*S. cerevisiae*	Sf9 insect cells (*S. frugiperda*)	Lardizabal et al. (2001)
UeDGAT2	*U. ramanniana*	Sf9 insect cells (*S. frugiperda*)	Lardizabal et al. (2001)

(Saha et al., 2006). Unlike other eukaryote enzymes, AhDGAT was purified from the soluble fraction of developing peanuts. Biosynthesis of TAG in the cytosol has been previously reported in a 10S multienzyme complex from the oleaginous yeast *Rhodotorula glutinis* (Gangar et al., 2001). Whether this soluble yeast DGAT and AhDGAT compose a novel class of DGATs is yet to be demonstrated.

1.3 MEMBRANE TOPOLOGICAL ORGANIZATION OF DGATs

The pattern in which a protein transverses the membrane bilayer is essential for elucidating the dynamics of the protein structure. DGAT1 and DGAT2 contain hydrophobic segments that are generally believed to constitute transmembrane domains (Fig. 1.1). DGAT1 displays more hydrophobic segments than DGAT2, which indicates a different topology and may relate to different physiological roles in TAG biosynthesis (Yen et al., 2008). Few experimental studies on DGAT topological organization in plants and yeast are available, and therefore we will mainly rely on *in silico* approaches to predict transmembrane segments and the orientation in the membrane bilayer.

A variety of web-based tools are available for predicting the topology of membrane proteins. Since only a few membrane proteins from bacteria are known to be beta-barrel shaped so far, the prediction algorithms are mostly developed for alpha-helical membrane proteins. Generally, five types of techniques have been used in these

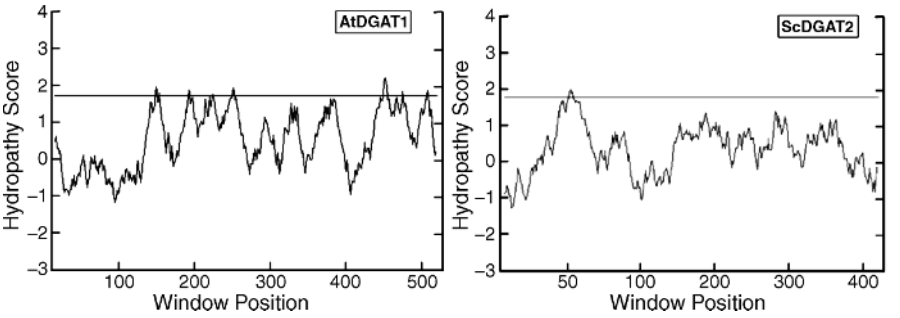

FIGURE 1.1 Kyte–Doolittle hydropathy plots of DGATs. Plots were generated by the method of Kyte and Doolittle (1982) using a window size of 19. Cutoff value (line) is 1.8 and peaks with score greater than 1.8 indicate possible transmembrane regions.

programs: hydrophobicity analysis combined with the positive inside rule (eg. TMpred and SOSUI), multiple sequence alignment (eg. ConPredII and TOPCONS), model-recognition approach (eg. MEMSTAT3, TMHMM, and HMMTOP), and support vector machine technique (eg. SVMtm) (Persson, 2006). An evaluation of the reliability of these methods indicated that a consensus prediction and model-based methods are best performing (Moller et al., 2001; Ikeda et al., 2002). The application of these algorithms for the prediction of TM domains in DGAT1 is described in Table 1.2 using AtDGAT1 and MmDGAT1 as models. For AtDGAT1, nine of the ten putative transmembrane domains are highly conserved among most of the prediction results except for the domains at 276–299 and 314–337 of AtDGAT1 and 251–276 and 285–312 of MmDGAT1 (highlighted TM5 and TM6 in Table 1.2). A model of nine-membrane-spanning topology agrees with our initial study on DGAT1 from *Brassica napus* (Foroud, 2005). In this work, protease mapping data showed that the region between 276 and 299 in BnDGAT1 (corresponding to TM5) is in the cytosol, in agreement with most of the prediction algorithms described in Table 1.2. Recent studies on DGAT1 from *Vernicia fordii* (tung tree) and *B. napus* indicated that the N-terminus faces the cytosolic side (Shockey et al., 2006; Weselake et al., 2006) as predicted by most algorithms in Table 1.2. The interaction of the N-terminus with lipid substrates in the cytoplasm may lead to a regulatory role of N-terminal region (Siloto et al., 2008) and there are several lines of evidence not only from *B. napus* DGAT1 but from mammalian DGAT1 and ACAT1 that favor this hypothesis (Cheng et al., 2001; Yu et al., 1999; Weselake et al., 2006). According to the work on VfDGAT1, the C-terminus of DGAT1 is also proved to orient toward cytosolic side, indicating an even number of membrane-spanning regions. This result disagrees with a nine-transmembrane topology model, and therefore further experimental testing will be required to examine the hypothesis of eight transmembrane domains.

Compared to DGAT1, DGAT2 is less hydrophobic, having a lower number of transmembrane domains and therefore a less intricate topology. The membrane topology of MmDGAT2 was experimentally determined revealing two transmembrane domains that are closely associated or a single hydrophobic domain embedded

TABLE 1.2 Prediction Results for Transmembrane Domains in DGAT1

	ConPredII	TOPCONS	MEMSAT3	HMMTOP	TMHMM	SVMtm	SOSUI	TMpred
AtDGAT1								
TM1	132–152	132–152	134–152	133–152	133–152	135–149	131–153	131–152
TM2	176–196	173–193	177–197	177–195	176–195	179–193	175–197	176–193
TM3	207–227	209–229	206–230	208–227	207–229	208–222	205–227	208–229
TM4	234–254	234–254	233–252	236–255	234–256	236–251	235–257	234–256
TM5	277–297	—	—	276–294	—	—	—	280–299
TM6	316–336	314–334	312–331	319–336	315–337	316–330	—	314–333
TM7	365–385	362–382	353–371	363–382	363–385	363–382	370–392	366–385
TM8	433–453	433–453	431–450	434–453	433–455	433–448	432–454	433–451
TM9	458–478	458–478	453–475	460–479	460–479	457–473	459–481	460–476
TM10	488–508	488–508	487–510	490–509	491–513	489–503	484–506	487–509
Orientation*	OUT	IN	IN	IN	IN	IN	N/A	OUT
MmDGAT1								
TM1	95–115	95–115	97–115	96–114	—	97–111	93–115	96–114
TM2	140–160	137–157	142–161	141–159	137–159	144–158	141–160	137–157
TM3	173–193	174–194	171–195	172–195	172–194	175–195	171–193	174–198
TM4	200–220	198–218	200–224	202–220	198–220	200–214	199–221	200–218
TM5	256–276	—	—	251–269	—	—	—	—
TM6	—	292–312	285–308	296–312	293–312	—		293–311
TM7	339–359	334–354	338–360	343–361	342–364	341–357	337–359	343–364
TM8	—	412–432	410–429	—	412–434	417–431	—	—
TM9	439–459	434–454	432–456	439–456	439–456	439–454	—	436–456
TM10	465–485	465–485	464–483	467–484	463–485	467–481	—	463–483
Orientation*	IN	IN	IN	IN	OUT	N/A	OUT	IN

Note: The polypeptides corresponding to AtDGAT1 and MmDGAT1 were submitted to a number of transmembrane prediction algorithms. The numbers correspond to the position of each transmembrane (TM) domain.

*Orientation of N-terminus. Cytosol: "IN". Lumen: "OUT". TMs highlighted in gray are not universally predicted. The websites used for each algorithm are: ConPred II, http://bioinfo.si.hirosaki-u.ac.jp/~ConPred2; TOPCONS, http://topcons.net; MEMSAT3, http://bioinf.cs.ucl.ac.uk/psipred/psiform.html; HMMTOP, http://www.enzim.hu/hmmtop; TMHMM, http://www.cbs.dtu.dk/services/TMHMM; SVMtm, http://ccb.imb.uq.edu.au/svmtm; SOSUI, http://bp.nuap.nagoya-u.ac.jp/sosui; TMpred, http://www.ch.embnet.org/software/TMPRED_form.html.

in the membrane bilayer (Stone et al., 2006). The first transmembrane domain (TM1) of MmDGAT2 and ScDGAT2 was ubiquitously predicted, but the second (TM2) was identified by only a few algorithms (Table 1.3). Since the homology of DGAT2 from different organisms is lower than that of DGAT1, it is possible that ScDGAT2, which has a distinct hydropathy plot, could have a different topology compared with other fungi DGAT2s. This could be demonstrated by the prediction results of *Schizosaccharomyces pombe* SpDGAT2 (Table 1.3). Interestingly, the prediction of N-terminus orientation seems to be related to the length of the predicted N-terminal tail. DGAT2s with putative long tails are intended to face toward the cytosol, which agrees with work on VfDGAT2 and MmDGAT2 (Shockey et al., 2006; Stone et al., 2006). The same conclusion, however, cannot be made for DGAT2s with short tails.

1.4 ALIGNMENT OF DGAT1 POLYPEPTIDES

DGAT1 polypeptides are typically characterized by a hydrophilic N-terminus sequence followed by a number of hydrophobic stretches constituting potential transmembrane domains as previously discussed. The total number of predicted transmembrane domains in DGAT1 can vary according to the sequence and the algorithm used as shown above. When the sequences are aligned, however, many of these potential transmembrane domains are found in the same positions in most DGAT1 (Fig. 1.2). The first four transmembrane domains on the first half of the sequences and the last three transmembrane domains on the C-terminus are separated by short polar loops. Between these groups are two possible membrane-spanning regions that are separated by longer hydrophilic stretches. Here we will consider these nine potential transmembrane domains as landmarks to describe conserved motifs in DGAT1, acknowledging, however, that an experimental approach is required to verify these assumptions. We will also use the sequence of *A. thaliana* DGAT1 to describe the exact position of each motif.

An overview of the DGAT1 alignment from 30 different organisms indicates several conserved regions with about 7% of identical residues among plant and animal sequences. The hydrophilic N-terminus is composed of an average of 115 and 80 residues in plants and animals, respectively and is the least conserved region in DGAT1. An alignment of the N-terminal portion of DGAT1 from a broad range of organisms revealed a cluster of arginines in the first 30 residues (Fig. 1.3). The region comprising 20 positions preceding the first hydrophobic domain is also conserved and contains the motifs PAHRXXXESPLSSDAIFXQ and SLFSXXSGFXN, which are conserved in plants and animals, respectively. Other divergences discriminating DGAT1 from plants and animals include a serine at position 131 of AtDGAT1 conserved in plants and absent in animal DGAT1, and the motif WVXRQ in plants, corresponding to FL($^{L}/_{I}$)($^{R}/_{K}$)R in animals. These differences can be also observed in more ancient organisms such as *Toxoplasma gondii* and *Physcomitrella patens*. The long loop between the fourth and fifth transmembrane domains (between positions 260 and 278 of AtDGAT1) shows remarkable variability among all DGAT1s. Following this region lies the most conserved uninterrupted sequence of DGAT1

TABLE 1.3 Prediction Results for Transmembrane Domains in DGAT2

	ConPredII	TOPCONS	MEMSAT3	HMMTOP	TMHMM	SVMtm	SOSUI	TMpred
ScDGA2								
TM1	73–93	62–82	59–77	68–92	70–92	66–97	75–97	72–92
TM2	—	84–104	80–104	—	—	—	—	—
TM3	189–209	188–208	—	—	—	193–207	188–210	196–214
TM4	215–235	—	—	200–224	—	217–231	213–234	216–236
TM5	293–313	—	—	294–310	—	—	—	—
TM6	—	—	—	341–359	—	—	—	—
Orientation	IN	IN	IN	IN	IN	IN	N/A	IN
MmDGAT2								
TM1	70–90	71–91	61–85	68–92	73–95	73–93	66–88	76–96
TM2	—	93–113	88–112	—	—	95–109	93–115	—
TM3	—	—	160–178	—	—	—	—	—
TM4	—	—	—	—	—	—	—	224–248
Orientation	IN	IN	IN	IN	IN	OUT	N/A	IN
AtDGAT2								
TM1	19–39	20–40	18–36	19–42	15–37	19–43	16–38	27–50
TM2	44–64	43–63	39–60	47–64	39–61	45–60	44–65	—
TM3	109–129	—	103–121	112–129	—	112–126	—	112–130
TM4	134–154	—	—	—	—	138–153	136–153	134–154
Orientation	OUT	IN	IN	IN	OUT	OUT	N/A	OUT
SpDGAT2								
TM1	29–49	29–49	26–45	32–51	—	29–43	25–47	—
TM2	54–74	51–71	48–72	60–77	49–65	46–70	53–75	49–65
TM3	115–135	—	119–137	115–134	115–137	119–133	—	115–137
TM4	141–161	—	—	143–162	142–162	—	136–153	142–162
TM5	217–237	—	—	217–236	217–237	—	—	217–237
TM6	—	—	—	259–278	—	—	—	—
Orientation	OUT	IN	IN	IN	OUT	OUT	N/A	OUT

Note: The polypeptide corresponding to ScDGAT2, MmDGAT2, AtDGAT2, and SpDGAT2 were submitted to a number of transmembrane prediction algorithms. The numbers correspond to the position of each transmembrane (TM) domain.

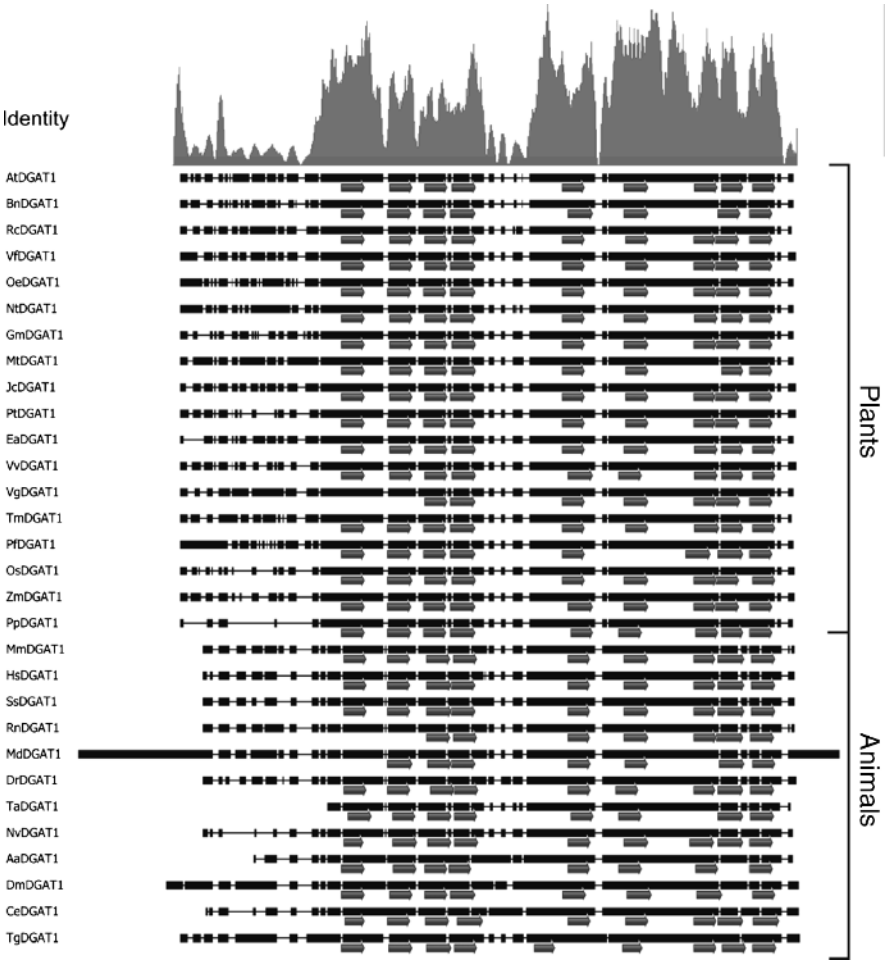

FIGURE 1.2 Alignment of transmembrane domains in DGAT1. The putative transmembrane domains of DGAT1 polypeptides from 12 animal and 18 plant organisms were predicted and the polypeptides were aligned. The identity of the alignment is graphed on the top using a window size of 6. The arrows denote the predicted transmembrane domains. The thick lines represent the sequence of each DGAT1, and the thin lines represent the gaps generated by the alignment. The picture was generated with Geneious Pro 4.6.0 and optimized manually. The transmembrane domains were predicted with transmembrane hidden Markov model (TMHMM). Accession numbers for the DGAT1 polypeptides are: AtDGAT1, NM_127503; AaDGAT1, XP_001658299; BnDGAT1, AAD45536; CeDGAT1, CAB07399; DmDGAT1, AAL78365; DrDGAT1, NP_956024; EaDGAT1, AAV31083; GmDGAT1, AAS78662; HsDGAT1, NP_036211; JcDGAT1, ABB84383; MdDGAT1, XP_001371565; MmDGAT1, NP_034176; MtDGAT1, ABN09107; NtDGAT1, AAF19345; NvDGAT1, XP_001639351; OeDGAT1, AAS01606; OsDGAT1, BAD53762; PfDGAT1, AAG23696; PpDGAT1, XP_001770929; PtDGAT1, XP_002330510; RcDGAT1, AAR11479; RnDGAT1, BAC43739; SsDGAT1, NP_999216; TaDGAT1, XP_002112025; TgDGAT1, AAP94209; TmDGAT1, AAM03340; VfDGAT1, ABC94471; VgDGAT1, ABV21945; VvDGAT1, CAN80418; ZmDGAT1, ABV91586.

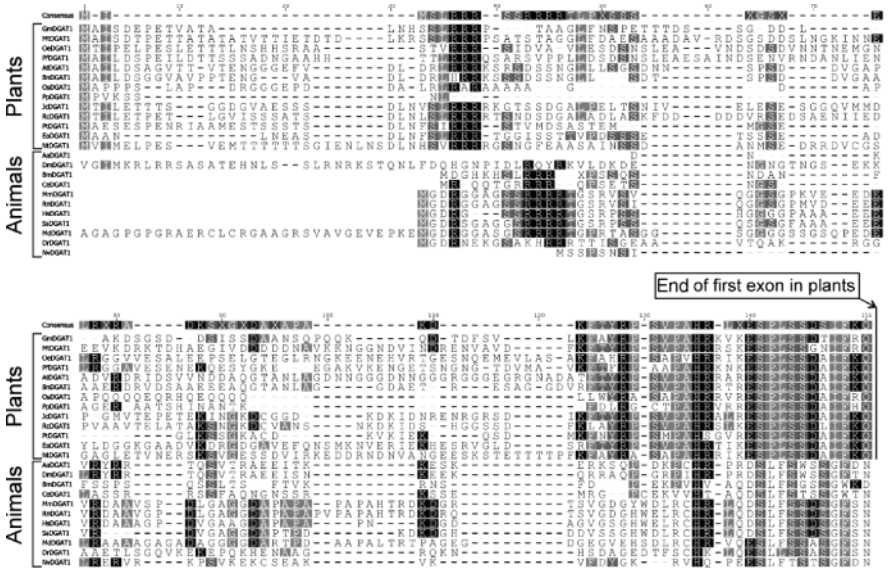

FIGURE 1.3 Alignment of the N-terminus polypeptide sequence of DGAT1 from plants and animals. Gray shades denote the polarity of blocks of conserved residues. The position corresponding to the end of the first exon in plants is indicated.

comprising the motifs PTLCYQXSYPR in plants and PTLCYEXXFPR in animals, preceding the fifth predicted transmembrane domain between positions 292 and 297 of AtDGAT1.

1.5 ALIGNMENT OF DGAT2 POLYPEPTIDES

DGAT2 polypeptides, in comparison to DGAT1, display fewer potential transmembrane domains and higher sequence divergence. An alignment of DGAT2 sequences from 20 organisms, covering plants and animals previously described in DGAT1, indicate approximately 5% of identical residues. Inclusion of 16 fungi sequences in this group decreases the identity to only 2.3%. A higher divergence might pose difficulties for identification of novel members of DGAT2 through sequence homology.

At least one transmembrane domain can be predicted for every DGAT2, but usually two transmembrane domains are conserved in the N-terminus portion and separated by a small loop (Fig. 1.4). This hydrophobic region is definitely very important because its removal results in lack of activity in ScDGAT2 (unpublished). An experimental approach indicated that the only membrane-spanning region in MmDGAT2 is composed of two transmembrane domains separated by a small loop that could be also interpreted as a single hydrophobic region embedded in the

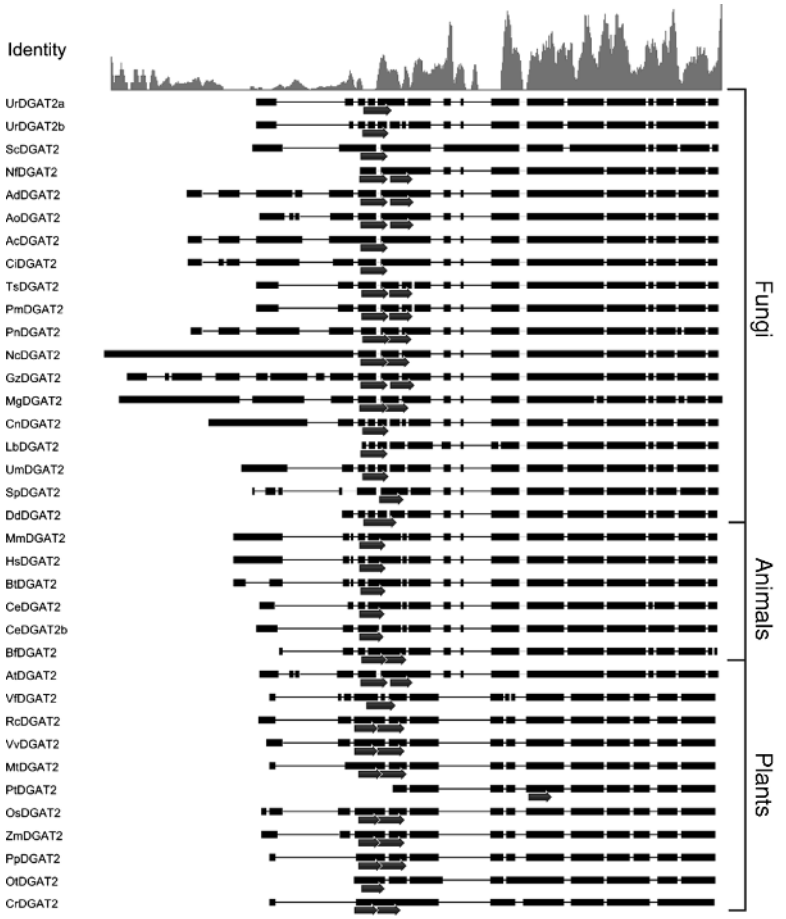

FIGURE 1.4 Alignment of transmembrane domains in DGAT2. The putative transmembrane domains of DGAT2 polypeptides from 18 fungi, 5 animals, and 11 plants were predicted and the polypeptides were aligned. The identity of the alignment is graphed on the top using a window size of 6. The arrows denote the predicted transmembrane domains. The thick lines represent the sequence of each DGAT2 polypeptide, and the thin lines represent the gaps generated by the alignment. The picture was generated as described for DGAT1. Accession numbers for the DGAT2 polypeptides are: AcDGAT2, XP_001540241; AdDGAT2, XP_001273210; AnDGAT2, CAK46407; AoDGAT2, XP_001822244; AtDGAT2, NP_566952; BfDGAT2, XP_002208225; BtDGAT2, CAD58968; CeDGAT2, CAB04533; CeDGAT2b, AAB04969; CiDGAT2, XP_001240299; CnDGAT2, EAL20089; CrDGAT2, XP_001693189; DdDGAT2, XP_635762; GzDGAT2, XP_381525; HsDGAT2, AAK84176; LbDGAT2, EDR14458; MgDGAT2, XP_368741; MmDGAT2, AAK84175; MtDGAT2, ACJ84867; NcDGAT2, CAE76475; NfDGAT2, XP_001261291; OsDGAT2, NP_001057530; OtDGAT2, CAL58088; PmDGAT2, XP_002146410; PnDGAT2, EAT89076; PpDGAT2, XP_001777726; PtDGAT2, XP_002317635; RcDGAT2, AAY16324; ScDGAT2, NP_014888; SpDGAT2, XP_001713160; TsDGAT2, EED21737; UmDGAT2, XP_760084; UrDGAT2a, AAK84179; UrDGAT2b, AAK84180; VfDGAT2, ABC94474; VvDGAT2, CAO68497; ZmDGAT2, ACG38122.

membrane (Stone et al., 2006). This region will be used as a landmark and the positions of conserved motifs also will be indicated in the UrDGAT2a polypeptide from *U. ramanniana*. The N-terminus portion preceding the transmembrane domains is quite variable in length and is usually smaller in animals and plants (with 38 and 30 residues in average, respectively) when compared with fungi (with 100 residues in average). The most conserved region in DGAT2 encompasses the motif RXGFX($^{K}/_{R}$) XAXXXGXX($^{L}/_{V}$)VPXXXFG($^{E}/_{Q}$) located approximately 150 residues after the second transmembrane domain (positions 259–281 of UrDGAT2a). Other conserved residues are the motif GGXXE (positions 204–208 in UrDGAT2a) and a phenylalanine, an arginine, and a proline in positions 164, 170, and 293 of UrDGAT2a, respectively. In addition, the motif YXXXXXHPHG is conserved in sequences from animals and fungi (positions 121–129 of UrDGAT2a) corresponding to YXXXXXEPH$^{S}/_{G}$ in plants. Preceding this motif is situated one of the most striking divergences in DGAT2 alignment, a hydrophilic segment of approximately 41 residues present in sequences from some fungi but absent in plants and animals. This region, corresponding to positions 144–185 of ScDGAT2, is also found as a much larger segment (158 residues) in *Yarrowia lipolytica* DGAT2. This hydrophilic segment, although nonessential, was demonstrated to modulate the enzyme activity of ScDGAT2 (unpublished results). Because this segment precedes a highly conserved motif, it is possible that it might represent a specialized function in DGAT2 from certain fungi.

1.6 STRUCTURE OF DGAT GENES

The architecture of genes encoding DGAT is largely available from whole-genome sequence databases or, as in the case of *V. fordii*, from sequencing of the respective genomic regions. In mammals, genes encoding DGAT1 share a similar architecture of 17 exons mostly grouped in the 3′ portion. A *DGAT1* representative from invertebrates (*Caenorhabditis elegans*), however, shows an unrelated distribution with only seven exons (Fig. 1.5A). In plants, DGAT1 genes from *A. thaliana*, *M. truncatula*, *Z. mays*, and *V. fordii* are composed of 16 exons, while DGAT1 from *O. sativa* contains 14 exons (Fig. 1.5B). The first exon of plant *DGAT1* genes comprises the largest coding sequence and encodes the hydrophilic N-terminus. Curiously, the last codon from the first exon of these genes encodes a glutamine in the same position of the alignment (motif IFX**Q**), denoting the end of the hydrophilic N-terminus and start of the first predicted membrane-spanning region (Fig. 1.3). The hydrophilic N-terminus is the most variable sequence of DGAT1 polypeptides, and therefore it is possible that segregation of this sequence in the first exon might have been used as an evolutionary mechanism to delimit variability in this region of the gene. This pattern was not observed in *DGAT1* sequences from animals. *DGAT2* genes show a structure that is dissimilar to that of *DGAT1*. Mammalian *DGAT2* genes share a common architecture with eight exons while the gene from *C. elegans* has only two exons (Fig. 1.5C). In plants *DGAT2* genes have eight exons in *A. thaliana* and ten exons in *V. fordii* and *O. sativa* (Fig. 1.5D).

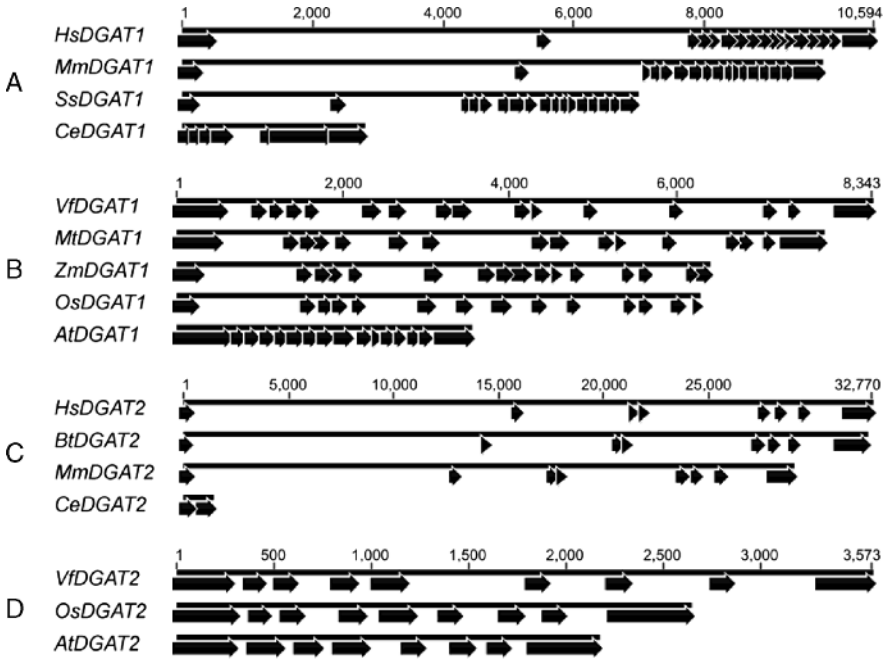

FIGURE 1.5 Architecture of DGAT genes. (A) *DGAT1* from animals, (B) *DGAT1* from plants, (C) *DGAT2* from animals, and (D) *DGAT2* from plants. The genomic sequences of each DGAT are represented by black bars. The arrows correspond to the regions comprising the coding region of the mRNA. The numbers correspond to the nucleotide positions. Accession numbers are: *HsDGAT1*, AC_000140.1; *MmDGAT1*, NC_000081.5; *SsDGAT1*, AY116586.1; *CeDGAT1*, NC_003283.9; *VfDGAT1*, DQ356679.1; *MtDGAT1*, AC174465.2; *ZmDGAT1*, AM433916.2; *OsDGAT1*, AP008212.1; *AtDGAT1*, NC_003071.4; *HsDGAT2*, NC_000011.8; *BtDGAT2*, NC_007313.3; *MmDGAT2*, NC_000073.5; *CeDGAT2*, Z81557.1; *VfDGAT2*, DQ356681.1; *OsDGAT2*, AP004757.3 and *AtDGAT2*, NC_003074.5.

1.7 FUNCTIONAL MOTIFS IN DGAT1

Most of the information available on the structure and function of DGATs is derived from comparisons of homologous enzymes. Alignments of polypeptide sequences encoding acyl-CoA-dependent acyltransferases from diverse organisms indicated a conserved histidine and an aspartic acid in the configuration **H**XXXX**D**. Substitution of the conserved histidine in the bifunctional enzyme 2-acyl-glycerophosphoethanolamine acyltransferase/acyl–acyl carrier protein synthase (Aas, EC 2.3.1.40 and 6.2.1.20, respectively) resulted in lack of acyltransferase activity (Heath and Rock, 1998). Substitution of the aspartic acid residue also resulted in significantly less activity. It was suggested that the histidine operates as a general base to abstract the proton from the hydroxyl group of the *sn*-1 glycerol-3-phosphate, facilitating nucleophilic attack on the thioester bond of acyl-CoA. The aspartic acid would work

in a charge relay system to increase the nucleophilicity of the hydroxyl group. This mechanism could be used by other acyltransferases, including DGAT. In fact a similar motif (**HH**XXX**DG**) is conserved in DGATs from prokaryotes (Daniel et al., 2004). In eukaryotic DGAT1, the motif **H**XXX**D** can be found closely after the fourth predicted transmembrane domain in DGAT1 from plants (positions 257–261 of AtDGAT1). Similarly, the motif **H**XXXX**D** is found in a region preceding the fifth predicted transmembrane domain of a few plants such as *A. thaliana*, *B. napus*, *R. communis*, and *V. fordii* (positions 342–347 of AtDGAT1) (Fig. 1.6). These motifs, however, are not conserved in animals and therefore might not compose the catalytic site of DGATs. Jako et al. (2001) identified the consensus sequence N(S/A/G)**R**(L/V)(I/F/A)(I/L)**E**N(L/V) in AtDGAT1 and proposed that the invariant arginine and glutamic acid on positions 149 and 153 could have functions analogous to those of histidine and aspartic acid residues, respectively. This region is highly conserved in all organisms including more ancient eukaryotes (*T. gondii* and *P. patens*) (Fig. 1.6). These residues

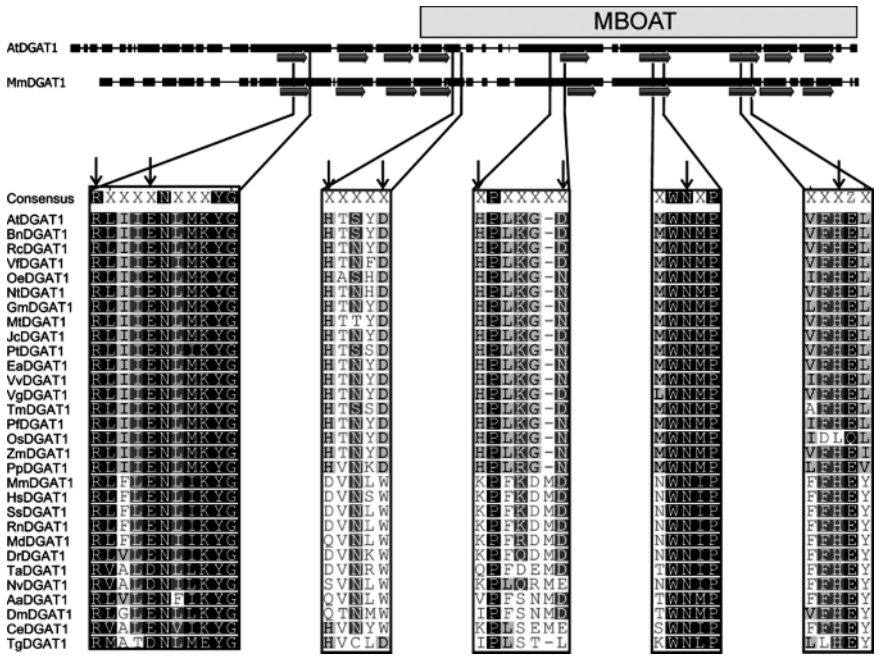

FIGURE 1.6 Alignment of putative active sites in DGAT1. A scheme MmDGAT1and AtDGAT1 is described on the top with the position of the MBOAT motif. The arrows in this scheme represent the predicted transmembrane domains. The thick lines represent the sequence of each DGAT1 polypeptide, and the thin lines represent the gaps generated though the alignment as previously shown. The vertical boxes contain the amino acid sequences for different DGATs indicated on the left. The arrows on these boxes indicate the position of conserved residues discussed in the text. Accession numbers for the DGAT polypeptides are the same as in Figure 1.2.

are present in the interface between a putative transmembrane domain and the adjacent hydrophilic loop, which would create an amphipathic environment for the substrates of DGAT. Moreover, DGAT1 is recognized as a member of a large protein family of membrane-bound O-acyltransferases known as MBOAT (NCBI domain ID pfam03062; Hofmann, 2000). Other members of the MBOAT family catalyze O-acylation reactions transferring acyl chains onto hydroxyl or thiol groups of lipids and proteins. For example, ACAT transfers an acyl chain from acyl-CoA to cholesterol, forming cholesteryl esters (Chang et al., 1993) while skinny hedgehog (ski) protein transfers a palmitoyl group onto cysteine residues of other proteins (Chamoun et al., 2001). The MBOAT family is characterized by a hydrophobic region (positions 234–509 of AtDGAT1) that contains a conserved asparagine (position 410 in AtDGAT1) and histidine (position 447 in AtDGAT1) (Fig. 1.6). It has been proposed that these residues could be involved in the catalytic activity. For example, this conserved histidine has been demonstrated to be a key residue for human ACAT1 activity (Guo et al., 2005). Whether any of these regions contribute to the catalytic site of DGAT1 is yet to be experimentally tested. Interestingly, *sn*-1 glycerol 3-phosphate acyltransferase (GPAT, EC 2.3.1.15) and lysophosphatic acid acyl transferase (LPAAT, EC 2.3.1.51), which are also membrane-bound O-acyltransferases catalyzing the first two acylation steps of TAG biosynthesis, are not classified as MBOAT members, suggesting that these enzymes might not share similar catalytic sites. It is also possible that these residues could act as supplementary catalytic sites being involved in other enzyme activities besides DGAT, such as ARAT and ACAT.

Other putative active sites in DGAT1 include the substrate binding sites. Sequences of DGAT1 from several plants indicate the presence of a putative diacylglycerol/phorbol ester binding motif that is apparently absent in ACATs (Zou et al., 1999; Nykiforuk et al., 2002; Xu et al., 2008). Phorbol esters such as phorbol-12-myristate-13-acetate (PMA) are commonly known to mimic diacylglycerols. The putative diacylglycerol/phorbol ester binding motif present in the positions 414 and 424 of AtDGAT1 forms the consensus **H**XXXX**RH**XXX**P** in DGAT1 from plants and animals. Xu et al. (2008) demonstrated that substitution of a phenylalanine by an arginine in position 439 of TmDGAT1 that is 16 positions after the predicted motif resulted in loss of DGAT activity. This could be a result of alterations in DAG interaction with DGAT. But, because this phenylalanine is positioned at a predicted transmembrane domain, substitution by a charged residue could also have structural implications. Acyl-CoA has been shown to interact with a recombinant N-terminal segment of BnDGAT1 and MmDGAT1 (Weselake et al., 2000, 2006; Siloto et al., 2008). The N-terminus sequence is highly variable, except for a region of 20 residues preceding the first hydrophobic domain, which shows remarkable conservation among plants and animals. Many of these variations, however, represent amino acid residues with similar properties, which could explain the acyl-CoA binding properties of DGAT1 from *B. napus* and *M. musculus*. Several lines of evidence suggest that acyl-CoA interaction with the hydrophilic N-terminus of DGAT1 regulates this enzyme allosterically. First, there is positive cooperativity exhibited for binding of 22:1-CoA in mouse and canola DGAT1 (Weselake et al., 2000; Siloto et al., 2008). Second, enzymes that are allosterically regulated

often form multimeric complexes to achieve cooperativity and the N-terminus of DGAT1 assists in the formation of dimers and tetramers as demonstrated for BnDGAT1 and HsDGAT1, respectively (Weselake et al., 2006; Cheng et al., 2001). For example, ACAT1 self-associates through the N-terminus, which also plays a regulatory role in this enzyme (Guo et al., 2001; Yu et al., 2002). Third, the acyl-CoA binding motif is not essential for enzyme activity because the removal of the N-terminus of RcDGAT1 results in a polypeptide with substantial enzyme activity, indicating that this is not the exclusive region to interact with acyl-CoA (unpublished data). Indeed, the fourth conserved block in GPATs and LPAATs, as described by Lewin et al. (1999), contains an invariant proline that has been proposed to participate in acyl-CoA binding. This proline was identified in plant DGAT1 polypeptides on the third predicted transmembrane domain corresponding to position 224 of AtDGAT1 and is in fact conserved in DGAT1 from all organisms. Substitution of this proline with an arginine in TmDGAT1 abolished DGAT activity, corroborating with the idea that this residue has a functional role (Xu et al., 2008). Another possible acyl-CoA binding site was proposed to be closely associated with the motif FYXDWWN in ACATs (Yen et al., 2008). This motif is present in DGAT1 and shows remarkable conservation with exception to CeDGAT1, where the second tryptophan is substituted by a phenylalanine. This motif is located on the loop preceding the third last putative transmembrane domain, relatively distant from the proline residue previously discussed, but near the asparagine residue conserved in MBOAT members. The paired tryptophans in this motif are a rare combination and have been previously demonstrated to participate in cholesterol binding. Guo et al. (2001) demonstrated, however, that substitution of the conserved tyrosine by alanine in yeast ACAT1 resulted in decreased affinity for acyl-CoA. Substitution of this same residue in TmDGAT1 (Y392A) resulted in decreased enzyme activity while a double mutation in tyrosine and tryptophan (Y392G/W395G) completely abolished enzyme activity (Xu et al., 2008).

Other putative functional domains predicted in DGAT1 include a leucine zipper and phosphorylation sites, although it is not yet clear whether these regions are important in the function, structure, or regulation of DGAT1. A putative leucine zipper motif was described in several DGAT1 from plants (Bouvier-Nave et al., 2000a; Nykiforuk et al., 2002). For example, in AtDGAT1 polypeptides five leucines (L222, L229, L236, L243, and L250) are consecutively spaced by six residues forming a classic leucine zipper (Hobbs et al., 1999). This leucine zipper, which might mediate interactions with other proteins, is present in a number of DGAT1 from plants but not from animals. Several studies indicated the presence of multiple potential phosphorylation sites in DGAT1 (Hobbs et al., 1999; Nykiforuk et al., 2002; He et al., 2004). Some of these sites are conserved in plant DGATs, such as the protein kinase C sites in the loop between the first and second transmembrane domains (positions 169–171 and 172–175 of AtDGAT1) and the casein kinase II sites (positions 254–257 and 403–406 of AtDGAT1). In addition, a tyrosine kinase site (positions 386–393 of AtDGAT1) is conserved in DGAT1 from plants and animals. This site overlaps with the FYXDWWN motif previously discussed as a putative acyl-CoA binding site. Although substitution of the conserved tyrosine by alanine in yeast

ACAT homologue resulted in lower affinity to acyl-CoA, phosphorylation could not be directly detected (Guo et al., 2001). Regulation of DGAT1 activity through phosphorylation is compelling not only because this is a common mechanism to control enzyme activity in eukaryotes but also because DGAT can scavenge DAG, an important molecule involved in phosphorylation signaling cascades (Carrasco and Merida, 2007). For example, the affinity of DAG to C1 domains of DAG kinase is modified by phosphorylation of residues situated close to this motif (Thuille et al., 2005). In addition, the fact that DGAT is expressed in vegetative tissues suggests that it can have additional roles beyond oil biosynthesis in seeds (Lu et al., 2003). Substitution of serine at position 168 in RcDGAT1 that corresponds to a protein kinase C site previously described resulted in a significant decrease in the enzyme activity (unpublished).

1.8 FUNCTIONAL MOTIFS IN DGAT2

The motifs previously described for DGAT1 cannot be found in DGAT2 sequences likely due to the little homology between DGAT1 and DGAT2. In fact, little is known about functional motifs of DGAT2. Stone et al. (2006) identified the conserved motif HPHG in positions 161–164 of MmDGAT2 as an important region for DGAT activity. Substitution of these residues, forming the sequences **A**PHG, H**G**HG, HP**A**G, and **AGA**G, resulted in a significant reduction of enzyme activity. More specifically, the histidine at position 163 of MmDGAT2 appeared to play a more important role for the enzyme function, which agrees with our mutagenesis work on ScDGAT2 (unpublished). This region is conserved in animal and fungi DGAT2, but in plants this motif is found as $EPH^{S}/_{G}$. Substitution of the glutamic acid by a histidine residue in plant DGAT2 did not result in an appreciable effect, but replacement of the motif HPHG in ScDGAT2 with residues EPHS found in plant DGAT2 resulted in loss of enzyme activity (unpublished). This indicates an important divergence on the structure/function of DGAT2 from fungi and plants. In addition, the motif $FLXLXXX^{n}$ (n indicates a nonpolar residue) was indicated as a putative neutral lipid binding domain in MmDGAT2 (Stone et al., 2006). Substitution of phenylalanine (position 80) and leucine (position 81) residues by alanine residues resulted in decreased DGAT activity. Substitution of the leucine in position 83 by an alanine resulted in lack of activity. This motif, present in the first predicted transmembrane domain of MmDGAT2 (positions 80–87), is conserved in vertebrate DGAT2 but not in plants or fungi orthologs. Substitution of the corresponding phenylalanine and leucine (positions 71 and 73) in ScDGAT2 results in a decrease of approximately 50% of the wild-type activity (unpublished). This same motif contains the putative membrane lipid attachment LGVAC found in prokaryotes through the interaction between the sulfhydryl group of a cysteine residue (position 87 of MmDGAT2) and DAG. Substitution of this cysteine by a serine in MmDGAT2 did not reduce DGAT activity, indicating that it does not function as a lipid attachment site. In fact, substitution of all cysteine residues in ScDGAT2 by alanine residues did not disrupt DGAT activity, indicating that this mechanism of DAG interaction is not present or at least essential in

this enzyme (unpublished data). In addition, substitutions on the conserved motif YFP located close to the transmembrane domains (positions 104–106 of UrDGAT2A) resulted in significant decreases in the enzyme activity.

1.9 SUBCELLULAR LOCALIZATION OF DGATs

To better elucidate the role of DGATs in cellular processes, their spatial location has been studied in different plants. In numerous earlier studies, DGAT location has been a subject of discrepancy whether it is associated with ER or oil bodies (Lung and Weselake, 2006). This debate could be the result of technique limitations because the general approach used in these studies was subcellular fractionation combined with enzyme assay in which cross-contamination can occur. For instance, in the study of germinating soybean cotyledon, the purified oil bodies also exhibited activities for ER markers (Settlage et al., 1995). This could be explained by association between oil bodies and ER (Cao and Huang, 1986; Settlage et al., 1995). Lacey and Hills (1996) applied different organelle markers to rule out the possible contamination in the assay and clearly demonstrated that *B. napus* DGAT is associated with ER. Similarly, Cao and Huang (1986) were able to localize maize DGAT in the rough ER (RER) by taking advantages of protein markers as well as the attachment of RER with polysomes in the presence of Mg^{2+} during fractionation. Actually the ER is regarded as the main site for TAG synthesis, and microsomal fractions from developing seeds of many plants as well as plant cultured cells have been extensively utilized for enzyme assays (Browse and Somerville, 1991; Weselake, 2005). Using more dependable techniques such as green fluorescent protein (GFP)-tagging and immunofluorescence, Shockey et al. (2006) have demonstrated that tung tree DGAT1 and DGAT2 are localized in the ER. Localization of both DGATs is dependent on a C-terminal ER retrieval motif. In VfDGAT1, the ER retrieval sequence YYHDL is part of the motif LLYYHDXMN conserved in all plant DGAT1. The ER retrieval domain in VfDGAT2 comprises the sequence LKLEI, where the two leucines are conserved in other DGAT2 sequences. Removal of the corresponding regions through C-terminus truncations in RcDGAT1 and ScDGAT2 resulted in decreased activity and decreased protein stability, respectively, indicating the importance of the C-terminus portion for both DGATs (unpublished). Interestingly, VfDGAT1 and VfDGAT2 do not colocalize in the ER, and therefore it is plausible that these polypeptides have distinct interactions with other proteins in the ER membrane. Mounting evidence based on studies with animals and plants indicate that DGAT1 and DGAT2, although catalyzing the same enzyme activity, have distinct physiological functions (Yen et al., 2008; Shokey et al., 2006; Burgal et al., 2008). In addition to the ER, DGAT activity was also found in chloroplasts of spinach leaves (Martin and Wilson, 1984) and more recently, Kaup et al. (2002), identified DGAT1 in the chloroplasts of senescing *Arabidopsis* leaves through immunoblotting. The mechanisms by which AtDGAT1 is transported to the chloroplast are yet to be determined.

In yeast, biochemical studies with *S. cerevisiae* indicated that DGAT activity is mainly in lipid droplets (Sorger and Daum, 2002). Indeed, DGAT2 in *U. rammaniana*

was purified from the lipid particle fractions (Lardizabal et al., 2001). In addition, two subcellular localization datasets generated by proteomic studies of *S. cerevisiae* indicated that ScDGAT2 localizes in ER and lipid droplets (Huh et al., 2003; Natter et al., 2005). Moreover, recombinant expression of ScDGAT2 in a yeast strain devoid of TAG biosynthesis indicated that ScDGAT2 localizes in the microsomal fraction as an integral membrane protein (unpublished). Due to the presence of conserved transmembrane domains, it is expected that yeast DGAT2 localizes in the ER. The mechanisms involved in its movement from the ER to lipid droplets, however, are not yet determined. *S. cerevisiae* lipid droplets contain a small fraction of proteins (Leber et al., 1994) when compared to the structurally related organelles in plants that are coated by oleosins (Tzen et al., 1993). The mechanism of oil body targeting in oleosins has been well studied and is assisted by a long hydrophobic domain composed of two chains that are separated by a motif with three conserved prolines (proline knot motif) that supposedly folds the domain, resulting in an unusual topological structure where the hydrophilic N- and C-termini face the cytoplasm (Tzen et al., 1992; Abell et al., 2004). Analysis of yeast DGAT2 revealed that the two potential transmembrane domains are separated by a very small loop. This region contains three prolines that are conserved in most sequences (Fig. 1.7). Such

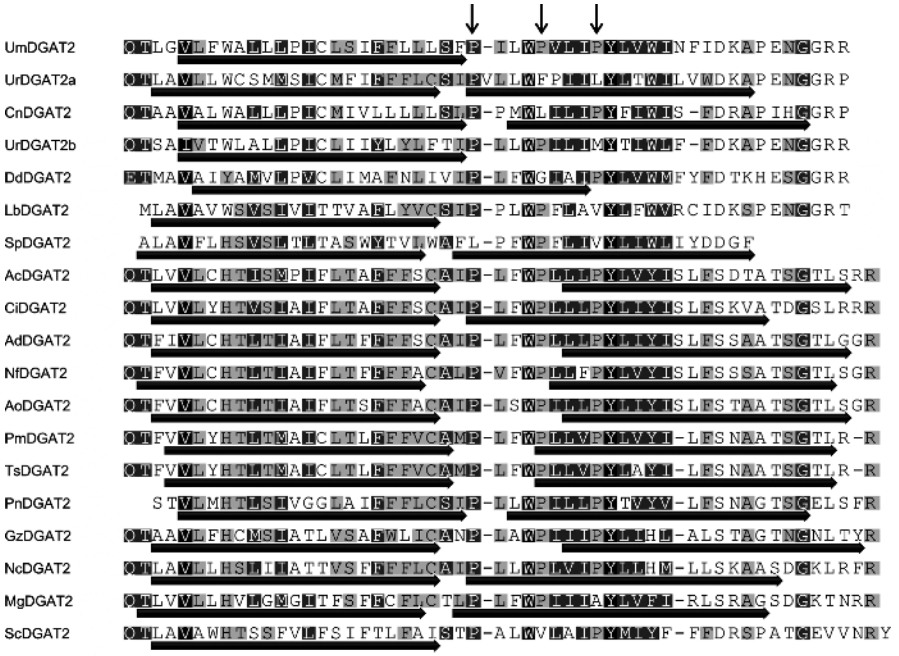

FIGURE 1.7 Alignment of the predicted transmembrane domain region from fungi DGAT2. Residues are highlighted in different shades of gray to black according to their similarity. The arrows denote the position of the predicted transmembrane domains. The positions of prolines conserved in many sequences are denoted by the arrows on the top. The alignment parameters and the accession numbers are the same as previously indicated in Figure 1.4.

similarities could explain the transfer of DGAT2 to lipid droplets, although this hypothesis needs to be experimentally verified. A study on murine DGAT2 has shown that the enzyme localizes on the ER and transfers to near the surface of lipid droplets when oleic acid is provided to drive TAG biosynthesis (Stone et al., 2009). Interestingly, determination of murine DGAT2 topological structure also showed both termini facing the cytosol and the possible presence of two adjacent transmembrane domains (Stone et al., 2006). DGAT2 from other organisms have a similar structure. VfDGAT2 has both N- and C-termini facing the cytosol with two predicted transmembrane domains separated by a small loop with a conserved proline (Shockey et al., 2006).

1.10 CONCLUSIONS AND FUTURE RESEARCH

Considerable progress has been achieved toward our understanding of DGATs and their involvement in the biosynthesis of TAG over the past decade. Many important aspects of the molecular mechanisms coordinating the catalytic activity, however, remain unclear. Most interestingly, DGAT1 and DGAT2 are unrelated polypeptides and yet catalyze the same reaction. Are the mechanisms involved in the acyltransferase catalytic function similar in DGAT1 and DGAT2? Are there any relationships between these enzymes that have not been identified with the current alignment algorithms? In an evolutionary perspective, did these enzymes evolve separately to catalyze the same reaction or do they have a common ancestor? These are some unanswered questions that require more fundamental research on DGATs. It would be valuable to have insights into the three-dimensional structure of DGATs because it would help to resolve some of these doubts.

Most of the information on putative structure–function relationships in DGATs has been deduced using bioinformatic approaches. The conclusions obtained with such approaches are valuable but still require experimental validation. Considerable progress has been made in shedding light on the topological organization of murine DGAT2 (Stone et al., 2006). It would be interesting to conduct similar experiments with a fungal DGAT2, particularly with ScDGAT2. This polypeptide contains unique characteristics as previously discussed, making it an interesting candidate for structural studies. Moreover, the correct topology of DGAT1 should be experimentally evaluated to determine whether the nine- or ten-transmembrane model is the correct one. In addition, to enhance our knowledge on DGAT catalytic activity, broader studies involving site-directed mutagenesis should be performed to identify functional regions. Currently, two studies have been conducted with a plant DGAT1 (*T. Majus*) and an animal DGAT2 (*M. musculus*) evaluating the influence of only a few residues (Xu et al., 2008; Stone et al., 2006). The polypeptide alignments presented in this chapter indicate the presence of multiple sites that could be involved in the catalytic activity of DGAT. This type of research could greatly advance if random mutagenesis techniques such as directed evolution or site-saturation mutagenesis could be applied to DGATs. One of the obstacles associated with such large-scale experiments is that standard methods to accurately measure DGAT activity require a

laborious assay with radiolabeled substrates (Coleman, 1992). Due to the association of DGATs with membranes, enzyme assays typically use microsomal fractions obtained through ultracentrifugation, which greatly decreases the throughput of the assay. Recently, we have demonstrated two assays to detect and measure DGAT activity in high-throughput scale (Siloto et al., 2009). Further development of such assays would definitively enhance our knowledge about the molecular mechanisms involved in DGAT activity. Furthermore, this is an attractive field of plant biotechnology for improving the performance of DGATs from plants and fungi, which have been already used to increase oil content in seeds (Weselake et al., 2008; Lardizabal et al., 2008).

ACKNOWLEDGMENTS

The authors are grateful to the following grant agencies for funding in support of their DGAT characterization work: AVAC Ltd., Alberta Advanced Education and Technology, the Alberta Agricultural Research Institute, the Alberta Crop Industry Development Fund, the Canada Research Chairs Program, Genome Alberta, and the Natural Sciences and Engineering Research Council of Canada.

Abbreviations: EMS, ethyl methanesulfonate; TAG, triacylglycerol; DGAT, acyl-CoA:diacylglycerol acyltransferase; EST, expressed sequence tag; acyl-CoA: cholesterol acyltransferase, ACAT; ARAT, acyl-CoA:retinol acyltransferase; MGAT, acyl-CoA monoacylglycerol acyltransferase; TM, transmembrane; MBOAT, membrane-bound O-acyltransferases; PMA, phorbol-12-myristate-13-acetate; ER, endoplasmic reticulum; RER, rough ER; GFP, green fluorescent protein.

The two-character code preceding each DGAT gene and polypeptide indicates the organism of origin as follows:

Aa, *Aedes aegypti*; Ac, *Aspergillus clavatus*; Ah, *Arachis hypogaea*; An, *Aspergillus niger*; Ao, *Aspergillus oryzae*; At, *Arabidopsis thaliana*; Bf, *Branchiostoma floridae*; Bn, *Brassica napus*; Bt, *Bos taurus*; Ce, *Caenorhabditis elegans*; Ci, *Coccidioides immitis*; Cn, *Cryptococcus neoformans*; Cr, *Chlamydomonas reinhardtii*; Dm, *Drosophila melanogaster*; Dd, *Dictyostelium discoideum*; Dr, *Danio rerio*; Ea, *Euonymus alatus*; Gm, *Glycine max*; Gz, *Gibberella zeae*; Hs, *Homo sapiens*; Jc, *Jatropha curcas*; Lb, *Laccaria bicolor*; Md, *Monodelphis domestica*; Mm, *Mus musculus*; Mt, *Medicago truncatula*; Mg, *Magnaporthe grisea*; Nc, *Neurospora crassa*; Nf, *Neosartorya fischeri*; Nt, *Nicotiana tabacum*; Nv, *Nematostella vectensis*; Oe, *Olea europaea*; Os, *Oryza sativa*; Ot, *Ostreococcus tauri*; Pf, *Perilla frutescens*; Pm, *Penicillium marneffei*; Pn, *Phaeosphaeria nodorum*; Pp, *Physcomitrella patens*; Pt, *Populus trichocarpa*; Ps, *Picea sitchensi*; Rc, *Ricinus communis*; Rg, *Rhodotorula glutinis*; Rn, *Rattus norvegicus*; Sc, *Saccharomyces cerevisiae*; Sp, *Schizosaccharomyces pombe*; Ss, *Sus scrofa*; Ta, *Trichoplax adhaerens*; Tg, *Toxoplasma gondii*; Tm, *Tropaeolum majus*; Ts, *Talaromyces stipitatus*; Um, *Ustilago maydis*; Ur, *Umbelopsis ramanniana*; Vf, *Vernicia fordii*; Vg, *Vernonia galamensis*; Vv, *Vitis vinifera*; YL, *Yarrowia lipolytica*; Zm, *Zea mays*.

REFERENCES

Abell, B.M., Hahn, M., Holbrook, L.A., and Moloney, M.M. (2004) Membrane topology and sequence requirements for oil body targeting of oleosin. *Plant J.* 37, 461–470.

Bouvier-Nave, P., Benveniste, P., Noiriel, A., and Schaller, H. (2000a) Expression in yeast of an acyl-CoA:diacylglycerol acyltransferase cDNA from *Caenorhabditis elegans*. *Biochem. Soc. Trans.* 28, 692–695.

Bouvier-Nave, P., Benveniste, P., Oelkers, P., Sturley, S.L., and Schaller, H. (2000b) Expression in yeast and tobacco of plant cDNAs encoding acyl CoA:diacylglycerol acyltransferase. *Eur. J. Biochem.* 267, 85–96.

Browse, J., and Somerville, C. (1991) Glycerolipid synthesis-biochemistry and regulation. *Annu. Rev. Plant Physiol. Plant Molec. Biol.* 42, 467–506.

Burgal, J., Shockey, J., Lu, C.F., Dyer, J., Larson, T., Graham, I., and Browse, J. (2008) Metabolic engineering of hydroxy fatty acid production in plants: RcDGAT2 drives dramatic increases in ricinoleate levels in seed oil. *Plant Biotechnol. J.* 6, 819–831.

Cahoon, E.B., Shockey, J.M., Dietrich, C.R., Gidda, S.K., Mullen, R.T., and Dyer, J.M. (2007) Engineering oilseeds for sustainable production of industrial and nutritional feedstocks: solving bottlenecks in fatty acid flux. *Curr. Opin. Plant Biol.* 10, 236–244.

Cao, Y.Z., and Huang, A.H.C. (1986) Diacylglycerol acyltransferase in maturing oil seeds of maize and other species. *Plant Physiol.* 82, 813–820.

Carrasco, S., and Merida, I. (2007) Diacylglycerol, when simplicity becomes complex. *Trends Biochem. Sci.* 32, 27–36.

Cases, S., Stone, S.J., Zhou, P., Yen, E., Tow, B., Lardizabal, K.D., Voelker, T., and Farese, R.V. (2001) Cloning of DGAT2, a second mammalian diacylglycerol acyltransferase, and related family members. *J. Biol. Chem.* 276, 38870–38876.

Cases, S., Smith, S.J., Zheng, Y.W., Myers, H.M., Lear, S.R., Sande, E., Novak, S., Collins, C., Welch, C.B., Lusis, A.J., Erickson, S.K., and Farese, R.V. (1998) Identification of a gene encoding an acyl CoA:diacylglycerol acyltransferase, a key enzyme in triacylglycerol synthesis. *Proc. Natl. Acad. Sci. USA* 95, 13018–13023.

Chamoun, Z., Mann, R.K., Nellen, D., von Kessler, D.P., Bellotto, M., Beachy, P.A., and Basler, K. (2001) Skinny Hedgehog, an acyltransferase required for palmitoylation and activity of the Hedgehog signal. *Science* 293, 2080–2084.

Chang, C.C.Y., Huh, H.Y., Cadigan, K.M., and Chang, T.Y. (1993) Molecular cloning and functional expression of human acyl-Coenzyme A:cholesterol acyltransferase cDNA in mutant Chinese hamster ovary cells. *J. Biol. Chem.* 268, 20747–20755.

Cheng, D., Meegalla, R.L., He, B.K., Cromley, D.A., Billheimer, J.T., and Young, P.R. (2001) Human acyl-CoA:diacylglycerol acyltransferase is a tetrameric protein. *Biochem. J.* 359, 707–714.

Cheng, D., Nelson, T.C., Chen, J., Walker, S.G., Wardwell-Swanson, J., Meegalla, R., Taub, R., Billheimer, J.T., Ramaker, M., and Feder, J.N. (2003) Identification of acyl coenzyme A: Monoacylglycerol acyltransferase 3, an intestinal specific enzyme implicated in dietary fat absorption. *J. Biol. Chem.* 278, 13611–13614.

Coleman, R.A. (1992) Diacylglycerol acyltransferase and monoacylglycerol acyltransferase from liver and intestine. *Meth. Enzymol.* 209, 98–104.

Daniel, J., Deb, C., Dubey, V.S., Sirakova, T.D., Abomoelak, B., Morbidoni, H.R., and Kolattukudy, P.E. (2004) Induction of a novel class of diacylglycerol acyltransferases

and triacylglycerol accumulation in *Mycobacterium tuberculosis* as it goes into a dormancy-like state in culture. *J. Bacteriol.* 186, 5017–5030.

Dyer, J.M. and Mullen, R.T. (2008) Engineering plant oils as high-value industrial feedstocks for biorefining: the need for underpinning cell biology research. *Physiologia Plantarum* 132, 11–22.

Foroud, N.A. (2005) Probing the membrane topology of a diacylglycerol acyltransferase type I from Brassica napus, University of Lethbridge, Lethbridge, p. 194.

Gangar, A., Karande, A.A., and Rajasekharan, R. (2001) Isolation and localization of a cytosolic 10S triacylglycerol biosynthetic multienzyme complex from oleaginous yeast. *J. Biol. Chem.* 276, 10290–10298.

Guo, Z.M., Cromley, D., Billheimer, J.T., and Sturley, S.L. (2001) Identification of potential substrate-binding sites in yeast and human acyl-CoA sterol acyltransferases by mutagenesis of conserved sequences. *J. Lipid Res.* 42, 1282–1291.

Guo, Z.Y., Lin, S., Heinen, J.A., Chang, C.C.Y., and Chang, T.Y. (2005) The active site His-460 of human acyl-coenzyme A:cholesterol acyltransferase 1 resides in a hitherto undisclosed transmembrane domain. *J. Biol. Chem.* 280, 37814–37826.

He, X.H., Turner, C., Chen, G.Q., Lin, J.T., and McKeon, T.A. (2004) Cloning and characterization of a cDNA encoding diacylglycerol acyltransferase from castor bean. *Lipids* 39, 311–318.

Heath, R.J. and Rock, C.O. (1998) A conserved histidine is essential for glycerolipid acyltransferase catalysis. *J. Bacteriol.* 180, 1425–1430.

Hildebrand, D.F., Li, R., Hatanaka, T., and Stacey, G. (2008) Genomics of soybean oil traits. In: *Genetics and Genomics of Soybean*. Springer, New York, pp. 185–209.

Hobbs, D.H., Lu, C.F., and Hills, M.J. (1999) Cloning of a cDNA encoding diacylglycerol acyltransferase from *Arabidopsis thaliana* and its functional expression. *FEBS Lett*. 452, 145–149.

Hofmann, K. (2000) A superfamily of membrane-bound O-acyltransferases with implications for wnt signaling. *Trends Biochem. Sci.* 25, 111–112.

Huh, W.K., Falvo, J.V., Gerke, L.C., Carroll, A.S., Howson, R.W., Weissman, J.S., and O'Shea, E.K. (2003) Global analysis of protein localization in budding yeast. *Nature* 425, 686–691.

Ikeda, M., Arai, M., Lao, D.M., and Shimizu, T. (2002) Transmembrane topology prediction methods: a re-assessment and improvement by a consensus method using a dataset of experimentally-characterized transmembrane topologies. *In Silico Biol*. 2, 19–33.

Inokoshi, J., Kawamoto, K., Takagi, Y., Matsuhama, M., Omura, S., and Tomoda, H. (2009) Expression of two human acyl-CoA:diacylglycerol acyltransferase isozymes in yeast and selectivity of microbial inhibitors toward the isozymes. *J. Antibiot.* 62, 51–54.

Jako, C., Kumar, A., Wei, Y.D., Zou, J.T., Barton, D.L., Giblin, E.M., Covello, P.S., and Taylor, D.C. (2001) Seed-specific over-expression of an *Arabidopsis* cDNA encoding a diacylglycerol acyltransferase enhances seed oil content and seed weight. *Plant Physiol*. 126, 861–874.

Kalscheuer, R. and Steinbuchel, A. (2003) A novel bifunctional wax ester synthase/acyl-CoA: diacylglycerol acyltransferase mediates wax ester and triacylglycerol biosynthesis in *Acinetobacter calcoaceticus* ADP1. *J. Biol. Chem.* 278, 8075–8082.

Katavic, V., Reed, D.W., Taylor, D.C., Giblin, E.M., Barton, D.L., Zou, J.T., MacKenzie, S.L., Covello, P.S., and Kunst, L. (1995) Alteration of seed fatty-acid composition by an ethyl

methanesulfonate-induced mutation in *Arabidopsis thaliana* affecting diacylglycerol acyltransferase activity. *Plant Physiol.* 108, 399–409.

Kaup, M.T., Froese, C.D., and Thompson, J.E. (2002) A role for diacylglycerol acyltransferase during leaf senescence. *Plant Physiol.* 129, 1616–1626.

Kroon, J.T., Wei, Y.D., Simon, W.J., and Slabas, A.R. (2006) Identification and functional expression of a type 2 acyl-CoA:diacylglycerol acyltransferase (DGAT2) in developing castor bean seeds which has high homology to the major triglyceride biosynthetic enzyme of fungi and animals. *Phytochemistry* 67, 2541–2549.

Kyte, J. and Doolittle, R.F. (1982) A simple method for displaying the hydropathic character of a protein. *J. Molec. Biol.* 157, 105–132.

Lacey, D.J. and Hills, M.J. (1996) Heterogeneity of the endoplasmic reticulum with respect to lipid synthesis in developing seeds of *Brassica napus* L. *Planta* 199, 545–551.

Lardizabal, K., Effertz, R., Levering, C., Mai, J., Pedroso, M.C., Jury, T., Aasen, E., Gruys, K., and Bennett, K. (2008) Expression of *Umbelopsis ramanniana* DGAT2A in seed increases oil in soybean. *Plant Physiol.* 148, 89–96.

Lardizabal, K.D., Mai, J.T., Wagner, N.W., Wyrick, A., Voelker, T., and Hawkins, D.J. (2001) DGAT2 is a new diacylglycerol acyltransferase gene family—Purification, cloning, and expression in insect cells of two polypeptides from *Mortierella ramanniana* with diacylglycerol acyltransferase activity. *J. Biol. Chem.* 276, 38862–38869.

Leber, R., Zinser, E., Zellnig, G., Paltauf, F., and Daum, G. (1994) Characterization of lipid particles of the yeast. *Saccharomyces cerevisiae*. *Yeast* 10, 1421–1428.

Lewin, T.M., Wang, P., and Coleman, R.A. (1999) Analysis of amino acid motifs diagnostic for the sn-glycerol-3-phosphate acyltransferase reaction. *Biochemistry* 38, 5764–5771.

Li, F., Wu, X., Lam, P., Bird, D., Zheng, H., Samuels, L., Jetter, R., and Kunst, L. (2008) Identification of the wax ester synthase/acyl-coenzyme A:Diacylglycerol acyltransferase WSD1 required for stem wax ester biosynthesis in *Arabidopsis*. *Plant Physiol.* 148, 97–107.

Liang, J.J., Oelkers, P., Guo, C.Y., Chu, P.C., Dixon, J.L., Ginsberg, H.N., and Sturley, S.L. (2004) Overexpression of human diacylglycerol acyltransferase 1, acyl-CoA:cholesterol acyltransferase 1, or acyl-CoA:cholesterol acyltransferase 2 stimulates secretion of apolipoprotein B-containing lipoproteins in McA-RH7777 cells. *J. Biol. Chem.* 279, 44938–44944.

Lu, C.F.L., de Noyer, S.B., Hobbs, D.H., Kang, J.L., Wen, Y.C., Krachtus, D., and Hills, M.J. (2003) Expression pattern of diacylglycerol acyltransferase-1, an enzyme involved in triacylglycerol biosynthesis, in *Arabidopsis thaliana*. *Plant Molec. Biol.* 52, 31–41.

Lung, S.C. and Weselake, R.J. (2006) Diacylglycerol acyltransferase: A key mediator of plant triacylglycerol synthesis. *Lipids* 41, 1073–1088.

Martin, B.A. and Wilson, R.F. (1984) Subcellular localization of triacylglycerol synthesis in spinach leaves. *Lipids* 19, 117–121.

Moller, S., Croning, M.D.R., and Apweiler, R. (2001) Evaluation of methods for the prediction of membrane spanning regions. *Bioinformatics* 17, 646–653.

Milcamps, A., Tumaney, A.W., Paddock, T., Pan, D.A., Ohlrogge, J., and Pollard, M. (2005) Isolation of a gene encoding a 1,2-diacylglycerol-*sn*-acetyl-CoA acetyltransferase from developing seeds of *Euonymus alatus*. *J. Biol. Chem.* 280, 5370–5377.

Natter, K., Leitner, P., Faschinger, A., Wolinski, H., McCraith, S., Fields, S., and Kohlwein, S.D. (2005) The spatial organization of lipid synthesis in the yeast *Saccharomyces cerevisiae*

derived from large scale green fluorescent protein tagging and high resolution microscopy. *Molec. Cellular Proteom.* 4, 662–672.

Nykiforuk, C.L., Furukawa-Stoffer, T.L., Huff, P.W., Sarna, M., Laroche, A., Moloney, M.M., and Weselake, R.J. (2002) Characterization of cDNAs encoding diacylglycerol acyltransferase from cultures of *Brassica napus* and sucrose-mediated induction of enzyme biosynthesis. *Biochimica et Biophysica Acta Molec. Cell Biol. Lipids* 1580, 95–109.

Perry, H.J. and Harwood, J.L. (1993) Changes in the lipid content of developing seeds of *Brassica napus*. *Phytochemistry* 32, 1411–1415.

Persson, B. (2006) Bioinformatics in membrane protein analysis. In: Lundstrom, K.H., (ed.) *Structual Genomics of Membrane Proteins*. CRC Press, Florida, pp. 5–20.

Quittnat, F., Nishikawa, Y., Stedman, T.T., Voelker, D.R., Choi, J.Y., Zahn, M.M., Murphy, R. C., Barkley, R.M., Pypaert, M., Joiner, K.A., and Coppens, I. (2004) On the biogenesis of lipid bodies in ancient eukaryotes: synthesis of triacylglycerols by a *Toxoplasma* DGAT1-related enzyme. *Molec. Biochem. Parasitol.* 138, 107–122.

Saha, S., Enugutti, B., Rajakumari, S., and Rajasekharan, R. (2006) Cytosolic triacylglycerol biosynthetic pathway in oilseeds. Molecular cloning and expression of peanut cytosolic diacylglycerol acyltransferase. *Plant Physiol*. 141, 1533–1543.

Settlage, S.B., Wilson, R.F., and Kwanyuen, P. (1995) Localization of diacylglycerol acyltransferase to oil body associated endoplasmic reticulum. *Plant Physiol. Biochem.* 33, 399–407.

Shockey, J.M., Gidda, S.K., Chapital, D.C., Kuan, J.C., Dhanoa, P.K., Bland, J.M., Rothstein, S.J., Mullen, R.T., and Dyer, J.M. (2006) Tung tree DGAT1 and DGAT2 have nonredundant functions in triacylglycerol biosynthesis and are localized to different subdomains of the endoplasmic reticulum. *Plant Cell* 18, 2294–2313.

Siloto, R.M.P., Madhavji, M., Wiehler, W.B., Burton, T.L., Boora, P.S., Laroche, A., and Weselake, R.J. (2008) An N-terminal fragment of mouse DGAT1 binds different acyl-CoAs with varying affinity. *Biochem. Biophys. Res. Commun.* 373, 350–354.

Siloto, R.M.P., Truksa, M., Brownfield, D., Good, A.G., and Weselake, R.J. (2009) Directed evolution of acyl-CoA:diacylglycerol acyltransferase: Development and characterization of *Brassica napus* DGAT1 mutagenized libraries. *Plant Physiol. Biochem.* 47, 456–461.

Sorger, D. and Daum, G. (2002) Synthesis of triacylglycerols by the acyl-coenzyme A: diacylglycerol acyltransferase Dga1p in lipid particles of the yeast *Saccharomyces cerevisiae*. *J. Bacteriol.* 184, 519–524.

Stone, S.J., Levin, M.C., and Farese, R.V. (2006) Membrane topology and identification of key functional amino acid residues of murine acyl-CoA: diacylglycerol acyltransferase-2. *J. Biol. Chem.* 281, 40273–40282.

Stone, S.J., Levin, M.C., Zhou, P., Han, J.Y., Walther, T.C., and Farese, R.V. (2009) The endoplasmic reticulum enzyme DGAT2 is found in mitochondria-associated membranes and has a mitochondrial targeting signal that promotes its association with mitochondria. *J. Biol. Chem.* 284, 5352–5361.

Thuille, N., Heit, I., Fresser, F., Krumbock, N., Bauer, B., Leuthaeusser, S., Darnmeier, S., Graham, C., Copeland, T.D., Shaw, S., and Baier, G. (2005) Critical role of novel Thr-219 autophosphorylation for the cellular function of PKC theta in T lymphocytes. *EMBO J*. 24, 3869–3880.

Turkish, A.R., Henneberry, A.L., Cromley, D., Padamsee, M., Oelkers, P., Bazzi, H., Christiano, A.M., Billheimer, J.T., and Sturley, S.L. (2005) Identification of two novel human acyl-CoA wax alcohol acyltransferases: members of the diacylglycerol acyltransferase 2 (DGAT2) gene superfamily. *J. Biol. Chem.* 280, 14755–14764.

Tzen, J.T.C., Lie, G.C., and Huang, A.H.C. (1992) Characterization of the charged components and their topology on the surface of plant seed oil bodies. *J. Biol. Chem.* 267, 15626–15634.

Tzen, J.T.C., Cao, Y.Z., Laurent, P., Ratnayake, C., and Huang, A.H.C. (1993) Lipids, proteins, and structure of seed oil bodies from diverse species. *Plant Physiol.* 101, 267–276.

Weiss, S.B. and Kennedy, E.P. (1956) The enzymatic synthesis of triglycerides. *J. Am. Chem. Soc.* 78, 3550–3550.

Weiss, S.B., Kennedy, E.P., and Kiyasu, J.Y. (1960) Enzymatic synthesis of triglycerides. *J. Biol. Chem.* 235, 40–44.

Weselake, R.J. (2002) Biochemistry and Biotechnology of TAG Accumulation in Plants. In: Kuo, T.M. and Gardner, H.W., (eds.) *Lipid Biotechnology*, Peoria, IL: Marcel Dekker, pp. 27–56.

Weselake, R.J. (2005) Storage Lipids. In: Murphy, D.J., (ed.) *Plant Lipids: Biology, Utilization and Manipulation,* Oxford: Blackwell publishing, pp. 162–225.

Weselake, R.J., Madhavji, M., Szarka, S.J., Patterson, N.A., Wiehler, W.B., Nykiforuk, C.L., Burton, T.L., Boora, P.S., Mosimann, S.C., Foroud, N.A., Thibault, B.J., Moloney, M.M., Laroche, A., and Furukawa-Stoffer, T.L., (2006) Acyl-CoA-binding and self-associating properties of a recombinant 13.3 kDa N-terminal fragment of diacylglycerol acyltransferase-1 from oilseed rape. *BMC Biochem.* 7, 24–36.

Weselake, R.J., Nykiforuk, C.L., Laroche, A., Patterson, N.A., Wiehler, W.B., Szarka, S.J., Moloney, M.M., Tari, L.W., and Derekh, U. (2000) Expression and properties of diacylglycerol acyltransferase from cell-suspension cultures of oilseed rape. *Biochem. Soc. Trans.* 28, 684–686.

Weselake, R.J., Shah, S., Tang, M.G., Quant, P.A., Snyder, C.L., Furukawa-Stoffer, T.L., Zhu, W.M., Taylor, D.C., Zou, J.T., Kumar, A., Hall, L., Laroche, A., Rakow, G., Raney, P., Moloney, M.M., and Harwood, J.L. (2008) Metabolic control analysis is helpful for informed genetic manipulation of oilseed rape (*Brassica napus*) to increase seed oil content. *J. Exp. Botany* 59, 3543–3549.

Xu, J.Y., Francis, T., Mietkiewska, E., Giblin, E.M., Barton, D.L., Zhang, Y., Zhang, M., and Taylor, D.C. (2008) Cloning and characterization of an acyl-CoA-dependent diacylglycerol acyltransferase 1 (DGAT1) gene from *Tropaeolum majus*, and a study of the functional motifs of the DGAT protein using site-directed mutagenesis to modify enzyme activity and oil content. *Plant Biotechnol. J.* 6, 799–818.

Yen, C.L., Stone, S.J., Koliwad, S., Harris, C., and Farese, R.V. (2008) DGAT enzymes and triacylglycerol biosynthesis. *J. Lipid Res.* 49, 2283–2301.

Yen, C.L.E. and Farese, R.V. (2003) MGAT2, a monoacylglycerol acyltransferase expressed in the small intestine. *J. Biol. Chem.* 278, 18532–18537.

Yen, C.L.E., Monetti, M., Burri, B.J., and Farese, R.V. (2005) The triacylglycerol synthesis enzyme DGAT1 also catalyzes the synthesis of diacylglycerols, waxes, and retinyl esters. *J. Lipid Res.* 46, 1502–1511.

Yen, C.L.E., Stone, S.J., Cases, S., Zhou, P., and Farese, R.V. (2002) Identification of a gene encoding MGAT1, a monoacylglycerol acyltransferase. *Proc. Natl. Acad. Sci. USA* 99, 8512–8517.

Yu, C.J., Chen, J., Lin, S., Chang, C.C.Y., and Chang, T.Y. (1999) Human acyl-CoA:cholesterol acyltransferase-1 is a homotetrameric enzyme in intact cells and *in vitro*. *J. Biol. Chem.* 274, 36139–36145.

Yu, C.J., Zhang, Y., Lu, X.H., Chen, J., Chang, C.C.Y., and Chang, T.Y. (2002) Role of the N-terminal hydrophilic domain of acyl-coenzyme A:cholesterol acyltransferase I on the enzyme's quaternary structure and catalytic efficiency. *Biochemistry* 41, 3762–3769.

Yu, K., Li, R., Hatanaka, T., and Hildebrand, D. (2008) Cloning and functional analysis of two type 1 diacylglycerol acyltransferases from *Vernonia galamensis*. *Phytochemistry* 69, 1119–1127.

Zheng, P., Allen, W.B., Roesler, K., Williams, M.E., Zhang, S., Li, J., Glassman, K., Ranch, J., Nubel, D., Solawetz, W., Bhattramakki, D., Llaca, V., Deschamps, S., Zhong, G.Y., Tarczynski, M.C., and Shen, B. (2008) A phenylalanine in DGAT is a key determinant of oil content and composition in maize. *Nat. Genet.* 40, 367–372.

Zou, J.T., Wei, Y.D., Jako, C., Kumar, A., Selvaraj, G., and Taylor, D.C. (1999) The *Arabidopsis thaliana* TAG1 mutant has a mutation in a diacylglycerol acyltransferase gene. *Plant J.* 19, 645–653.